International Journal of Pharmaceutics 650 (2024) 123710

Contents lists available at ScienceDirect

International Journal of Pharmaceutics

journal homepage: www.elsevier.com/locate/ijpharm

Liposomal encapsulation of amoxicillin via microfluidics with subsequent investigation of the significance of PEGylated therapeutics

Edward Weaver [a,1], Robyn A. Macartney [a,b,1], Robyn Irwin [a], Shahid Uddin [c], Andrew Hooker [c], George A. Burke [b], Matthew P. Wylie [a], Dimitrios A. Lamprou [a,*]

[a] School of Pharmacy, Queen's University Belfast, 97 Lisburn Road, Belfast BT9 7BL, UK
[b] Nanotechnology & Integrated Bioengineering Centre (NIBEC), School of Engineering, Ulster University, York Street, Belfast BT15 1ED, UK
[c] Immunocore Ltd, 92 Park Dr, Milton, Abingdon OX14 4RY, UK

ARTICLE INFO

Keywords:
Microfluidics
Antibiotic
Antimicrobial resistance
Polyethylene glycol
Formulation
Liposome

ABSTRACT

With an increasing concern of global antimicrobial resistance, the efforts to improve the formulation of a narrowing library of therapeutic antibiotics must be confronted. The liposomal encapsulation of antibiotics using a novel and sustainable microfluidic method has been employed in this study to address this pressing issue, via a targeted, lower-dose medical approach. The study focusses upon microfluidic parameter optimisation, formulation stability, cytotoxicity, and future applications. Particle sizes of circa. 130 nm, with viable short-term (28-day) physical stability were obtained, using two different non-cytotoxic liposomal formulations, both of which displayed suitable antibacterial efficacy. The microfluidic method allowed for high encapsulation efficiencies (≈77 %) and the subsequent in vitro release profile suggested high limits of antibiotic dissociation from the nanovessels, achieving 90% release within 72 h. In addition to the experimental data, the growing use of poly (ethylene) glycol (PEG) within lipid-based formulations is discussed in relation to anti-PEG antibodies, highlighting the key pharmacological differences between PEGylated and non-PEGylated formulations and their respective advantages and drawbacks. It's surmised that in the case of the formulations used in this study, the addition of PEG upon the liposomal membrane would still be a beneficial feature to possess owing to beneficial features such as stability, antibiotic efficacy and the capacity to further modify the liposomal membrane.

1. Introduction

Antibiotic (AB) therapy is well-established for the treatment of various bacterial infections, with a diverse study finding that ABs were prescribed in between 77.4 and 350.3 times per 1000 primary care consultations in the UK (Van Staa et al., 2022). Despite their prevalence, ABs form a major concern for the healthcare community due to a lack of therapeutic effect and rising incidences globally of antimicrobial resistance (AMR), specifically antibacterial resistance. As a result of this, it appears that the pool of effective ABs is diminishing, with worries that AMR will lead to a state of total AB failure on a global scale.

Antimicrobial stewardship is a movement designed to reduce the causation of AMR, by the proper usage of ABs. This can be achieved by ensuring the correct AB is prescribed for the correct bacteria, with particular attention given to factors such as appropriate strength and regimen duration. A poignant means of reducing AMR is by treating the infection by using the highest possible dose of AB over the shortest duration of time (Bassetti et al., 2022). To reduce AMR though, it would be beneficial for the medicine to possess an element of targeted delivery, to prevent the action of the AB at unwanted sites. Current oral therapy, despite being implemented globally, requires excessively high doses of AB to be administered, due to a lack of target-specific delivery.

Another serious issue affecting the rise of AMR is the lack of patient compliance, which is prominent for antibacterial regimens. A 2021 study performed on patient adherence to antimicrobials found that just 13.03% of patients truly followed the correct prescribing regimen (Tong et al., 2018), indicating a chance that the therapy may be unsuccessful and cause a knock-on possibility for inducing AMR.

A method of improving patient compliance to a medical regimen can be by altering the drug delivery system (DDS) used to administer an active pharmaceutical ingredient (API), for example via the use of liposomes (LPs). LPs are vesicles sizing within the nano-micron range,

* Corresponding author.
E-mail address: D.Lamprou@qub.ac.uk (D.A. Lamprou).
[1] Authors contributed equally to this work.

https://doi.org/10.1016/j.ijpharm.2023.123710
Received 8 October 2023; Received in revised form 11 December 2023; Accepted 12 December 2023
Available online 13 December 2023

consisting at a base level of a lipid-based bilayer. LPs are capable of encapsulating both hydrophilic (Weaver et al., 2022b) and hydrophobic (Jaradat et al., 2022) APIs, making their usage potentially very attractive. The capacity to modify the surface of LPs, with moieties such as poly(ethylene glycol) (PEG) or protein conjugates can also provide the LPs with an element of targeted delivery. The capacity to localise the delivery of the API to a specific location reduces the dosage requirement and minimises delivery of the AB to non-essential target areas. This has been attributed to the reduction of AMR (Canaparo et al., 2019).

In addition, LPs have also been displayed to allow for prolonged release of an API. The majority of AB regimens consist of a multiple-dose-a-day medication over a number of days. This is via oral therapy, which is the preferred administration route; however, this type of regimen can be complex for certain population groups e.g., elderly, to adhere to and properly finish, which as mentioned is essential for proper AB efficacy. The potential to allow for a prolonged-delivery system via LPs, even if combined with other DDS systems, such as API-eluting scaffolds, could be a possible solution to improving patient compliance and AB therapy success.

Research on LP encapsulation of APIs has mainly been focussed on the encapsulation of therapeutic materials for cancer and vaccines (Weaver et al., 2022b; Jaradat et al., 2022), leaving the area of controlled release AB therapy relatively sparse (Weaver et al., 2021). There are currently few AB-based LP products available on the market, mostly due to the lack of research performed in the area, as well as the already established orally-administered activity seen in market-available medicines. Previous attempts at the encapsulation of ABs within LPs has seen pitfalls such as being time-consuming methods with poor control over particle characteristics (Wu et al., 2022), which leaves gaps in formulation space for emerging technologies (ETs), such as microfluidics (MFs), to address these issues.

MFs offers the opportunity to formulate various nanoparticle (NP) types, including lipid nanoparticles (LNPs), polymeric and metal colloids/inorganic (Volk et al., 2021; Baby et al., 2021). The precise control of fluids within sub-micron-sized channels by changing process parameters, including total flow rates (TFRs), flow rate ratios (FRRs) and capillary design, allows for the alteration of particle characteristics. MFs is also regarded as a sustainable procedure, both environmentally and economically, allowing for the formulation of nanomedicines in a time efficient manner, using a low volume of materials with reduced wastage (Weaver et al., 2022c). MFs has allowed for improving the encapsulation efficiency (EE) and physicochemical properties of LP formulations for various APIs, from biologics (Weaver et al., 2022b) to hydrophobic molecules (Ballacchino et al., 2021), to chemotherapeutics (Jaradat et al., 2022).

The material composition of the LP formulation has been seen to dramatically affect release kinetics and therapeutic efficacy, highlighting the importance of optimising the carrier vessel materials. A commonly used excipient for LNP formulation is PEG, which is used to enhance LP properties such as residence time, targeting and stealth properties (Zalba et al., 2022; Wang et al., 2023). The addition of PEGylated lipids within a formulation opens options for further LP modification, e.g., surface protein conjugation (Banerjee et al., 2022), as well as increasing static attractive forces, such as Van der Waals (VdW) forces which can supplement target specificity (Cannito et al., 2022).

PEGylated lipids are commonly used in combination with ionisable and cationic lipids for the delivery of mRNA; a prime example being the Covid-19 vaccine developed by various pharmaceutical companies. Their usage with anionic lipids, such as that which is used in this study is possibly less prevalent, but no less important. An optimal anionic-PEGylated LP formulation is far from being actualised, leading to the requirement for further research within this area to be performed.

Given the rise in interest of PEGylated lipids, there too has been a rise in the documentation of anti-PEG antibodies (APAs) (Ju et al., 2023), which may actually cause detrimental effects to the pharmacokinetics of a formulation via increased clearance and degradation. Due to this reason, within this study, a direct comparison between a PEGylated and non-PEGylated formulation is derived, to investigate whether PEG is essential for formulation efficacy.

This study acts as the first stepping-stone to the use of the MF method to produce antibacterial LPs, with a comparative analysis to examine the effect caused due to the use of PEG within an AB LP formulation. To the knowledge of the authors, the AB used in this study, Amoxicillin (AMOX) has yet to be explored via MF LP encapsulation, highlighting a gap in research that should be addressed.

2. Materials and methods

2.1. Materials

Cholesterol (Chol), and AMOX were purchased from Tokyo Chemical Industry (Tokyo, Japan). 1,2-Distearoyl-*sn*-glycero-3-phosphocholine (DSPC), phosphate buffered saline (PBS) tablets, ethanol (<99%), sodium phosphate monobasic (NaH_2PO_4), and acetic acid was purchased from Sigma-Aldrich (Poole, UK). N-(carbonyl-methoxypolyethylene glycol-2000)-1,2-distearoyl-*sn*-glycero-3-phosphoethanolamine, sodium salt (DSPE-PEG2K) was obtained from Lipoid (Ludwigshafen Germany). McCoy's 5A culture media with L-glutamine and Gentamicin were purchased from Lonza (Basel, Switzerland). Fetal bovine serum (FBS), heat inactivated South American origin and Trypsin EDTA were obtained from Gibco (Montana, US). Crystal violet and Sodium dodecyl sulfate was purchased from ThermoFisher (Massachusetts, US). Methanol and N,N-dimethylformamide (DMF) were purchased from ROMIL Ltd. (Cambridge,UK). 3-(4,5-dimethylthiazol-2-yl)-2,5-diphenyl tetrazolium bromide (MTT) was purchased from Invitrogen (Massachusetts, US). U-2 OS cell line, *Staphylococcus aureus* (*S. aureus*, ATCC 29213) and *Proteus mirabilis* (*P. mirabilis*, ATCC 51286) were purchased from ATCC (Virginia, US).

2.2. Preparation of amoxicillin-loaded LPs

LPs were fabricated via a MF method, employing LP self-assembly. The lipid phase used consisted of two different formulation bases, consisting of either the structural lipid DSPC (hereafter referred to as F1), or a combination of DSPE-PEG2K and DSPC (hereafter referred to as F2), alongside the bilayer stabilising agent, cholesterol. Total lipid concentration remained at 1 mg/ml, established in previous studies (Weaver et al., 2022b), using a 2:1 mass ratio (DSPC:Chol) for F1 and 2:2:2 (DSPC:DSPE-PEG2K:Chol) for F2. The aqueous phase consisted of PBS, dissolved with AMOX at concentrations of 0 (for empty LPs), 0.5, 1 and 2 mg/ml.

LPs were produced using 3D-printed "diamond-shaped" MF devices, as reported previously (Sommonte et al., 2022), altering the FRR to control the particle size obtained.

2.3. Dynamic light scattering

Dynamic light scattering (DLS) was performed using the Nanobook Omni particle sizer (Brookhaven Instruments, NY, USA). Each measurement was performed in triplicate with a total sample volume of 2 ml, using a dilution of 1 in 100. DLS was used to analyse particle size, polydispersity index (PDI) and zeta (ζ) potential.

2.4. Stability studies

Samples were produced and analysed via DLS on day 0 of preparation. Samples were divided into three groups in triplicate (total samples per formulation n = 9), kept at 5 °C, 21 °C and 37 °C and analysed subsequently on days 7, 14, 21 and 28 after preparation. Stability studies analysed particle size, PDI and ζ-potential. 5 °C and 21 °C mimicked storage conditions, whereas 37 °C represented physically stability post administration in vivo.

2.5. Fourier-transform infrared (FTIR) spectroscopy

FTIR was employed to further characterise chemical entities present within the formulation. Analysis was undertaken using an attenuated total reflection (ATR) module-FTIR spectrometer (Thermo fisher scientific, Nicolet IS50 FTIR with built in ATR) on solid samples obtained by centrifugation (30 min at 14,800 rpm). Samples were measured over a wave range of 4000–600 cm^{-1}, over 128 scans at a resolution of 4 cm^{-1} at an interval of 1 cm^{-1}. Any background absorption was subtracted prior to analysis.

2.6. In vitro drug release and encapsulation efficiency (EE)

To determine EE, LP formulations were centrifuged for 30 min at 14,800 rpm to separate an LP pellet from the suspension. The supernatant, containing any unencapsulated AMOX was removed and prepared for analysis. The remaining pellet was then washed with fresh PBS and subsequently removed for analysis, to ensure any free AMOX that was adhered onto the pellet surface was accounted for. Equation 1, was used to calculate EE.

$$Encapsulationefficacy(\%) = \frac{TotalWeightofAPIadded(mg) - WeightofUnencapsulatedAPI(mg)}{TotalWeightofAPIadded(mg)} \times 100$$

Equation 1. Calculation performed to obtain encapsulation efficiency for each formulation.

To perform in vitro release, the remaining pellet was resuspended in fresh PBS at 37 °C and placed into pre-prepared dialysis tubing (cellulose membrane, avg. flat width 10 mm, 0.4 in, MWCO 14,000, Sigma Aldrich). Dialysis tubing was then placed into 4 ml of fresh PBS at 37 °C to initiate release data. 0.5 ml Aliquots were taken at 0, 0.5, 1, 2, 3, 4, 24, 48 and 72 h, replacing the external media with 0.5 ml of fresh PBS at 37 °C after each 0.5 ml aliquot, to maintain sink conditions.

Reverse phase high performance liquid chromatography (HPLC) was used to determine AMOX concentration. The method used was adapted from Marcel et al. (2018). Briefly, a mobile phase of 0.2 M monobasic sodium phosphate (NaH2PO4) was used in isocratic flow through A C18 column (250 mm × 4.6 mm) from ThermoFisher scientific (MA, USA), at a flow rate of 1 ml/min, UV detection wavelength 278 nm, injection volume 50 µl. Compound calibration was obtained by serial dilution, obtaining an R = 1 trendline. Cumulative release data was then calculated.

2.7. Cell culture

U2OS cells were used as a model cell line and cultured in McCoy's 5A Medium with L-glutamine supplemented with 10% foetal bovine serum (FBS), and gentamicin sulphate (50 µg/ml). Cells were maintained in the growth phase, passaged at 70% confluence using 0.25% trypsin EDTA and maintained under normal cell culture conditions at 37 °C, 5% CO_2.

2.7.1. Cell attachment assay

Initial attachment was measured using a crystal violet assay. Cells were seeded at a density of $1x10^5$ cells/ml in media containing empty (control), DSPC/AMOX or DSPE-PEG/AMOX LPs and incubated at 37 °C, 5% CO_2 for 4 h before completion of the assay. Media was removed and samples were gently washed in PBS. Cells were fixed in ice cold, 20% methanol followed by incubation in 0.5% crystal violet solution. Samples were incubated at room temperature to facilitate staining for 30 min. The crystal violet solution was removed, and samples washed three times in deionised (DI) water to remove residual stain. Samples were incubated for 30 min under constant agitation in 10% acetic acid to solubilise the dye. Solubilised samples were aliquoted in triplicate in 96 well plates and optical density was read at 562 nm, after 20 s vigorous shaking to homogenise the solution, using a Tecan Spark microplate reader (Tecan, Switzerland). A total of 6 samples were analysed per experimental group and used for statistical analysis.

2.7.2. Cell viability assay

Cell viability was analysed using 3-(4,5-dimethylthiazol-2-yl)-2,5-diphenyl tetrazolium bromide (MTT). Cells were seeded at a density of $1x10^4$ cells/ml and allowed to adhere overnight at 37 °C, 5% CO_2 Spent media was removed from the samples, and they were washed in PBS before treatment with media containing empty (control), DSPC/AMOX or DSPE-PEG/AMOX LPs. Prior to dilution in cell culture media, the liposome solutions (prepared as previously described) were centrifuged, and supernatant was discarded to remove any trace of unencapsulated AMOX. Liposomes were then resuspended in cell culture media, filter sterilised (0.2 µm) and diluted to the required concentration. Samples were incubated at 37 °C, 5% CO_2, until predefined time points of 1, 3 and 7 days, media was aspirated and replaced at day 3. At each time point, MTT solution (5 mg/ml in PBS, filter sterilised) was added to a final concentration of 0.5 mg/ml and incubated at 37 °C until formazan crystals could be observed visually or under phase contrast. After removing culture media, a solubilisation buffer was added (20% SDS prepared in a 1:1 ratio of DMF: DI water, pH adjusted to 4.7 using acetic acid). Samples were briefly agitated in the dark until complete solubilisation of the formazan crystals. Following solubilisation samples were aliquoted in triplicate into a 96 well plate and absorbance was read at 572 nm after 20 s vigorous shaking to homogenise using a Tecan Spark microplate reader (Tecan, Switzerland). Cell inhibition is expressed as a percentage of the positive control samples cultured with no liposomal addition. Cell viability (%) was calculated using equation 2. A total of 6 samples were run per experimental group with results presented as mean ± standard deviation.

$$CellViability(\%) = \frac{Absorbance_{Sample} - Absorbance_{Blank}}{Absorbance_{PositiveControl} - Absorbance_{Blank}} \times 100$$

Equation 2. Calculation performed to obtain percentage cell viability. Where sample absorbance is the OD measured for each sample treated with liposomal formulations, blank absorbance is unstained cells with the solubilisation buffer and positive control absorbance is of untreated cells cultured on tissue culture plastic.

2.8. Bacterial studies

S. aureus, strain ATCC 29213 and *P. mirabilis*, strain ATCC 51286, were cultured in Mueller Hinton Broth (MHB) for 18 h under 37 °C orbital incubation at 100 rpm. All liposomal formulations and unencapsulated AMOX solutions were filter sterilised (0.2 µm) prior to use.

2.8.1. Minimum inhibitory concentration (MIC) and minimum bactericidal concentration (MBC) determination

MIC was investigated between the range of 194–1 µl/ml via serial dilution for F1, F2 and unencapsulated AMOX, using sterile 96-well plates. Bacterial solutions of 1×10^6 colony forming unit (CFU)/ml were prepared via dilution from a stock 1×10^8 CFU/ml in MHB and 100 µl of this was added to 100 µl of F1, F2, control LPs (empty) or free AMOX. The final concentration of bacteria per well was 5×10^5 CFU/ml.

A positive control of bacteria/MHB was prepared alongside a negative control of solely MHB. Plates were left for 18 h under 37 °C orbital incubation at 100 rpm. MIC was determined via visual determination of the lowest concentration with the absence of turbidity within the wells.

MBC was performed by plating any wells identified visually as clear onto Mueller Hinton (MH) Agar. 20 µl of each clear inoculation was plated and spread evenly across the agar surface. Plates were statically incubated for 24 h at 37 °C to allow for any potential colony growth if bacteria were present. Plates were assessed and MBC was determined using the limit of 99.9 % bacterial reduction. Experiments were performed using a 5 parallel dilution series and were performed a total of 3 times each.

2.8.2. Time kill assay

Time kill assay was performed using the same bacterial concentration as used to determine MIC and MBC, using a starting concentration of 1×10^5 CFU/ml after dilution within the wells. Well plates containing MHB with either free AMOX, F1 or F2 were incubated under orbital conditions at 37 °C. Concentrations of AMOX used were 1, 2 and 4 times the determined MIC. At time points of 2, 4 and 6 h, 20 µl of inoculation was withdrawn from the wells and diluted ten-fold in sterile PBS to minimise the incidence of antibiotic carry-over (Foerster et al., 2016). 20 µl of the diluted inoculation was then plated onto MH-agar and incubated statically for 18 h. CFU formed during the incubation were then counted and scaled up to compensate for dilution from the original broth, then plotted against time. Assays were performed in triplicate for all data collected.

2.9. Statistical analysis

Where appropriate, measurements were performed in triplicate, and data is presented as an average, with a representative ± standard deviation. Two-way ANOVA analysis was performed, when possible (GraphPad Prism 10), using significance limits of * ($p < 0.05$), ** ($p < 0.01$) and *** ($p < 0.001$).

3. Results and discussion

3.1. Particle Size, PDI and ζ potential

Particle size data obtained for AMOX formulations indicated a high propensity for effective AMOX-loaded liposomal formulation via MFs. As displayed in Fig. 1, all formulations obtained using a concentration of 0.5 and 1 mg/ml AMOX displayed particle sizes of <500 nm, over both FRRs tested. Increasing the concentration of API to 2 mg/ml caused the enlarging of both F1 and F2. This is likely to be attributed to the logP of AMOX, which is 0.87, suggesting a near complete association within the hydrophilic aqueous liposomal vacuole. As the cargo loading increases, a factor of steric hindrance on the phospholipid bilayer could be experienced, restricting the capacity for smaller vesicle formation.

The usage of DSPE-PEG2K within the formulation also allowed for the production of slightly smaller liposomes, as displayed by ANOVA analysis in Fig. 1a. This is a common trend observed in literature, caused by lateral repulsion forces between PEG chains, leading to an increased angle of curvature within the bilayer (Ghaferi et al., 2022).

The most significant effect coming from the particle size analysis can be attributed to the change in FRRs between 3:1 and 5:1. As seen in previous works, increasing the FRR from 3:1 to 5:1 has allowed for a decrease in particle size diameter, however at the consequence of increasing the PDI (Weaver et al., 2022a). This trend is similarly observed for the encapsulation of AMOX, although the PDI, whilst increasing, still remains below the desired 0.2 limit, indicative of a homogenous formulation. This factor is further reinforced by a statistically significant ($p < 0.05$) different particle size observed between flow rates used for both AMOX 1 and 2 mg/ml. The polydispersity variation between all formulation showed no significant differences, indicating that the MF method may be reproducible over a wide range of parameters. PDI is crucial to investigate, as it will affect factors such as drug release, adhesion properties and surface interaction (Tavares et al., 2021, Ekonomou et al., 2022). MFs is held in high regard for liposomal formulation as the technology is capable of producing formulations with well controlled PDI without the requirement of further post-processing. This isn't the case with more traditional NP formulation methods, such as

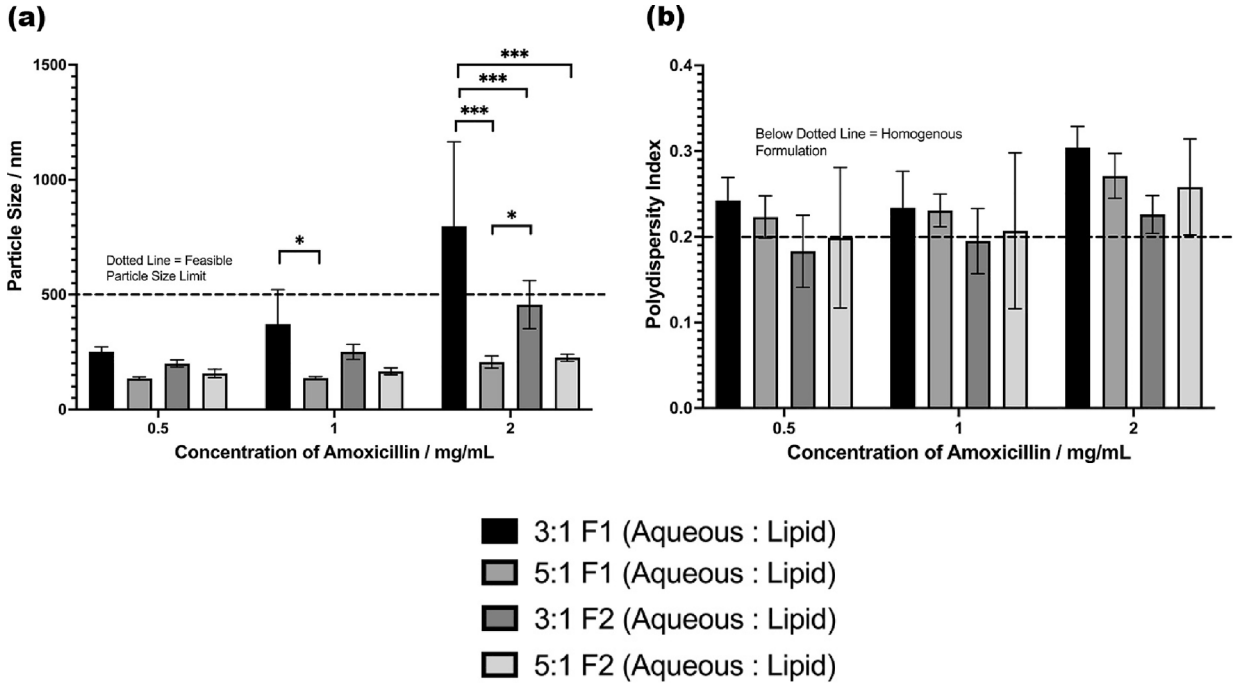

Fig. 1. (a) Particle size data shown for formulations over a range of 0.5, 1 and 2 mg/ml AMOX, using two carrier formulations over FRRs of 3:1 and 5:1 (Aqueous: Lipid) and (b) Polydispersity index data shown for formulations over a range of 0.5, 1 and 2 mg/ml AMOX, using F1 and F2 over FRRs of 3:1 and 5:1 (Aqueous: Lipid).

thin film hydration, which often requires the use of methods such as extrusion, to obtain a size and PDI-controlled NP. A cut-off for feasible particle size for these particles is proposed as 500 nm, as this renders the particles suitable for multiple administration routes including intravenous, transdermal, and intramuscular. For this specific study, the future use is intended for attachment to an additional DDS, such as electrospun fibres, which frequently have fibre diameters of around 1 μm.

In comparison to the blank liposomes assayed (using a 0 mg/ml AMOX concentration), as seen in figure SI 1, a negligeable difference in particle size and PDI was observed upon encapsulation, except for formulations containing 2 mg/ml AMOX, where the particle diameter increased significantly. From the data observed, lead formulation candidates would be identified by using an AMOX concentration of 1 mg/ml at a 5:1 FRR, for both F1 and F2. These formulations produce particle sizes of circa. 150 nm, with a well-controlled PDI.

The ζ-potential gives insight as to the surface electrostatic charge exhibited from the LPs. This will ultimately contribute to important factors within a formulation, such as physical stability and formulation pharmacokinetics. All lipids used in this formulation process were anionic, hence it was expected that the final LPs too would be anionic. This was confirmed by the data seen in Fig. 2. The influence of the API on the final ζ-potential of a formulation should be noted, as the addition of AMOX didn't statistically affect the overall particle charge upon encapsulation. This data is presented in figure SI 2. The surface charge may be more likely to be affected when using an API with higher logP values, such as testosterone or paclitaxel, as the API is present more within the LP bilayer, as opposed to the vacuole. Hence the electrostatic effect exhibited by the API is more influential (Chang et al., 2019).

In addition, comparing the ζ-potential of the F1 and F2 formulations, it's clear to see that the addition of a PEG surface moiety also alters the charge expressed on the surface of the LP. In the cases of all AMOX LPs, the ζ-potentials of the F2 formulations were statistically more negative as opposed to F1, especially at a 5:1 FRR. This is likely due to the PEG chain, which carries an inherent negative charge (Dave et al., 2019), causing an increase in electrostatic charge present from the membrane. This may suggest and contribute towards the prevention of aggregation during storage and post-administration; however, this will be examined further in the stability studies performed.

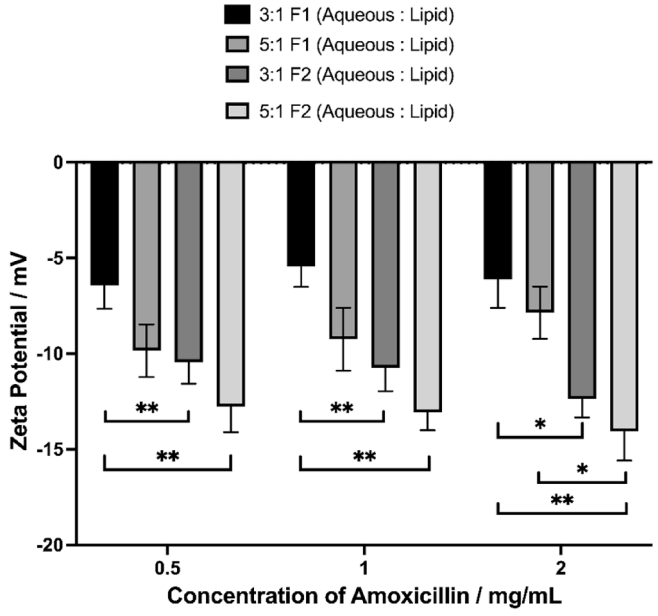

Fig. 2. ζ-Potential data shown for formulations over a range of 0.5, 1 and 2 mg/ml AMOX, using F1 and F2 formulations over FRRs of 3:1 and 5:1 (Aqueous: Lipid).

3.2. Stability studies

The physical stability of the formulations was examined to determine both how feasibly the formulation can be stored short term, as well as how the liposomes would interact post-administration. Upon observation of the data for F1, displayed in Fig. 3a, it's apparent that the formulations stored at 5 °C and 37 °C remained physically stable and viable over a 28-day period, whilst the particle size of the formulations stored at room temperature experienced a high degree of diameter increase. Whilst it may seem unusual that the two extreme temperatures allow for hospitable storage, and the intermediary storage causes significant change, an explanation may be possible. The increase in size of a formulation during storage is normally attributed to liposomal aggregation (Nakhaei et al., 2021), or in the case of protein eluting NPs, formation of a protein corona (Richtering et al., 2020). Neither F1 nor F2 have protein characteristics, hence the size increase is likely due to aggregation. At 21 °C, the cholesterol in the formulation, which plays a crucial role in the stability of a bilayer, interacts differently with the lipids than it would at both 5 °C and 37 °C. At higher temperatures, such as 37 °C, cholesterol reduces the fluidity of a membrane, reducing the ability of the membrane to deform and aggregate with other bilayers undergoing the same process (Kaddah et al., 2018). The DSPC bilayer itself won't undergo phase transition to a more-liquid like state until 55 °C (Chen et al., 2018), meaning that the determining factor for bilayer fluidity will be the influence of cholesterol. This provides evidence as to why F1 remained stable at 37 °C. At 5 °C, the DSPC membrane is far from reaching fluid-like properties, and the individual LPs possess less kinetic energy, due to their thermosensitive nature. This will mean that contact between LPs is unlikely to result in bilayer merging. However, at 21 °C, the cholesterol within the formulation is unlikely to cause sufficient membrane solidification to overcome the constant impacts between LPs. This will mean that merging of bilayers and subsequent aggregation into larger particles is possible. This increase in particle size will cause targeted clearance by the rough endoplasmic reticulum (RER), alleviating the formulation of any remaining efficacy.

The data presented in Fig. 3b, which depicts F2, suggests that all formulations that contain the PEG surface modification are stable over the three temperature conditions during the 28-day experiment. PEGylated lipids are often cited in literature to increase blood circulation half-life and decrease the incidences of aggregation of LP formulations (Zhang et al., 2016), due to a large increase in hydrophilicity and increased electrostatic repulsive forces exerted from the LP membrane, as seen in Fig. 2, displaying the increased negative ζ-Potential for PEGylated formulations. The ζ-Potential and PDI values obtained during the stability studies can be viewed in table SI 1&2. This trend is followed by the F2 LPs, whereby all stored formulations remained physically viable over the 28-day period. The PDI for most F2 formulations increased in the range of 0.1 during the storage period, suggesting a slight alteration in liposomal morphology. This would be likely to affect the efficacy of the formulation to a small extent, as a low PDI is often attributed to the predictability of the release profile (Maritim et al., 2021).

As seen in Fig. 3b, the sample stored at 21 °C appears to experience an increase in particle size beginning at day 21, which follows the trend observed in Fig. 3a, whereby the 21 °C LPs possessed the lowest level of stability in vitro, although F2 indicated a noticeable delay of aggregation onset when compared to F1.

From the data extrapolated, it appears that F2 possesses a higher propensity for stability, with suitable storage conditions at 5 °C and viable stability in simulated conditions post-administration.

3.3. Fourier transform infrared spectroscopy

FTIR was used to chemically characterise both F1 and F2 alongside the raw AMOX. The data is presented in Fig. 4. For spectra (a) and (b) in Fig. 4, the peaks at 2920 cm^{-1} and 2960 cm^{-1} are due to alkane

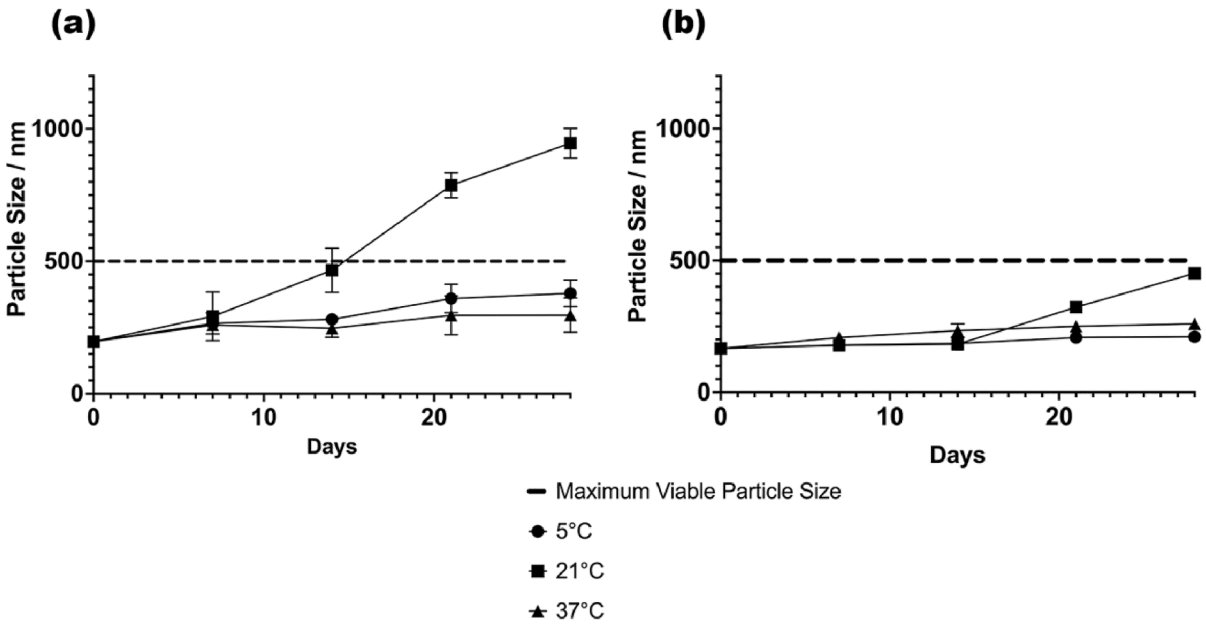

Fig. 3. Stability study data measuring particle size over a 28-day period. (a) Represents F1 and (b) F2. The line displayed at n = 500 is the maximum viable size for this formulation to be effective.

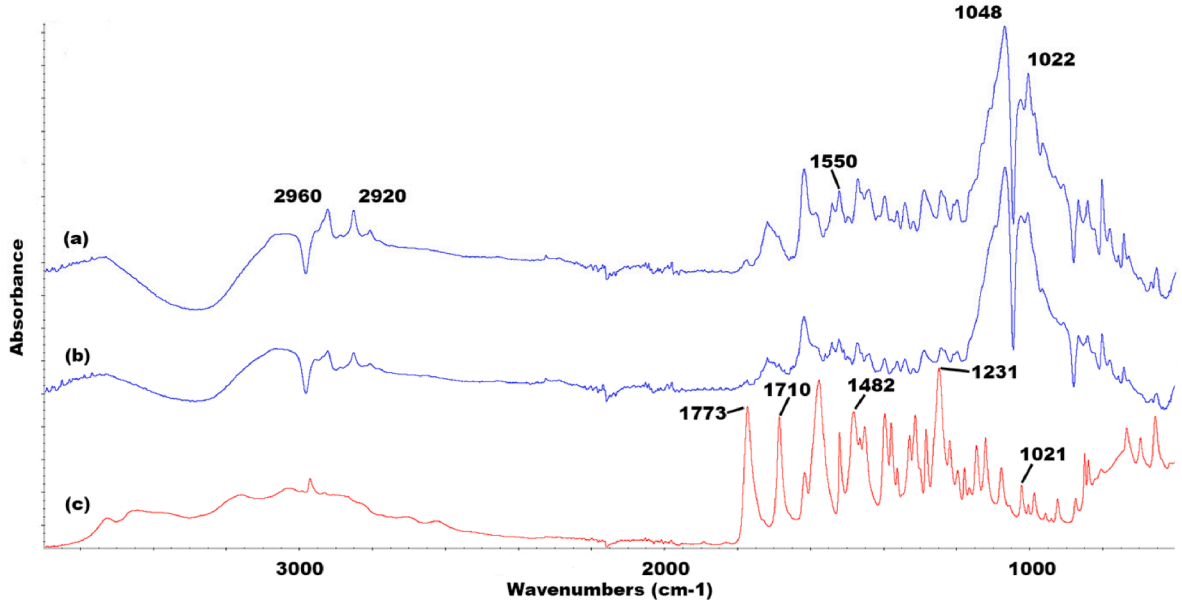

Fig. 4. FTIR Spectra for (a) F1, (b) F2 and (c) AMOX displayed between 3600 cm^{-1} and 600 cm^{-1}.

stretching within the lengthy hydrocarbon chains of the lipids, whilst the intense C–H bending causes the towering peak at 1022 cm^{-1}. This peak appears to be shifted slightly, which may be as a result of the C-O ester absorption which has been documented previously (Alinaghi et al., 2014). C-O-C stretching is present in the intense peak at 1048 cm^{-1}.

Unusually, the N–H primary amine stretching normally expected around 3500 cm^{-1} isn't present for (b), which may be attributed to overlapping absorption values from the AMOX (Vijayakumar et al., 2016), however, the characteristic primary amine in-plane scissoring vibrations at 1550 cm^{-1} are present.

Upon analysis of (c), the C=O stretch at 1773 cm^{-1} and C-N amide stretch at 1482 cm^{-1} are also present in (a) and (b), however the key identifier for confirming the presence of AMOX via IR is the C=O stretch occurring as a consequence of the AMOX β-lactam ring. The peak at 1231 cm^{-1} can be attributed to a combination of both C-N stretching and N–H bending upon consultation of literature (Bebu et al., 2011), whereas the aromatic C–N in the sulphide ring is more likely to be attributed to the peak at 1021 cm^{-1}, owing to the weak intensity of the peak.

3.4. Encapsulation efficiency and drug release

The encapsulation of AMOX, and the following release were investigated in vitro to provide information as to the effectiveness of MFs to prevent material wastage during manufacturing, and to produce a formulation capable of sufficient therapeutic API delivery. The EE produced was 77.43 ± 0.1 % and 78.3 ± 2.39% for F1 and F2 respectively, using a FRR of 5:1, which can be viewed in Fig. 5a. This is suggestive of similar levels of encapsulation displayed by other emerging methods such as supercritical assisted manufacturing (Trucillo et al., 2020), but is

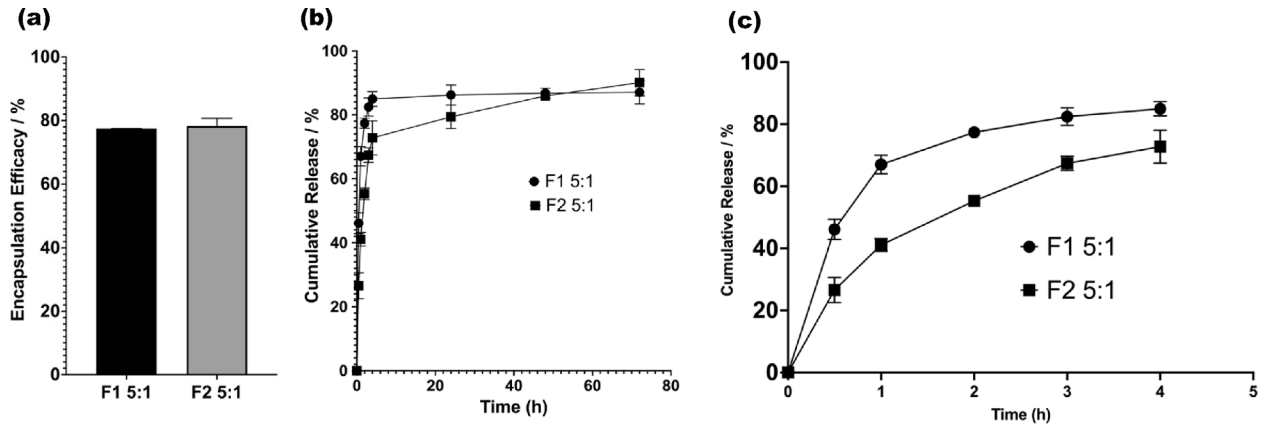

Fig. 5. (a) Encapsulation Efficiency for F1 and F2, using 1 mg/ml AMOX and a 5:1 FRR and (b) 72-hour release profiles for F1 and F2, using 1 mg/ml AMOX and a 5:1 FRR and (c) A detailed portrayal of the burst release exhibited in the first 4 h by F1 and F2.

much higher than traditional methods, such as film hydration, which has been shown in literature to encapsulate with only 28% efficiency (Patel et al., 2021).

The similarity of EEs between F1 and F2 is indicative that despite the differing charges and particle sizes, the loading of the API remains comparable. It was the original hypothesis of the authors that PEGylation would reduce the EE, owing to the isoelectric point of AMOX. AMOX has an isoelectric point of 4.7 (Radyukevich et al., 2019), meaning that below this value, the AMOX possesses a positive charge. The MF formulation method employed in this study manufactured LPs at pH 7.4, meaning that the AMOX would exist as a negatively charged entity. As a result, it was estimated that the more-negative PEGylated LPs would have a lower capacity for encapsulation. As a consequence of the results obtained, the comparable EEs suggest that the precision and speed of the self-assembly process that occurs via MFs negates the opposing charges and allows for efficient API encapsulation. The physical constraints imposed by the sub-micron channels, along with high pressure environment, appears to force the process of API encapsulation.

As previously mentioned, MFs is a sustainable technology, enabling the use of lower masses and concentrations of feedstocks (Weaver et al., 2022c). From an economic standpoint, AMOX is a low-cost drug compared to, for example, biologic APIs (Weaver et al., 2021), however, for all industrial processes, a high EE is preferred to reduce the cost of a manufacturing process. Considering the environmental impact though, the excessive wastage of ABs could have the chance to spread into the local ecosystem if left untreated post-processing, which could lead to disruption of life cycles and an increase of environmental AMR (González-Plaza et al., 2019).

The release profiles of both F1 and F2, Fig. 5b, both display a burst release profile. The PEGylation of the LPs, F2, appears to slow this burst release, indicated by the reduction in steepness of the datapoints shown in Fig. 5b. F1 appears to reach a plateau of AMOX release after just 4 h, whereas F2 burst releases to 70% within the 4-hour period then appears to provide a more controlled release over the next 48-hour period. Whether the concentration of API release over this last 48-hour period is sufficient for therapeutic effect will be explored within the bacterial studies. The reason for the reduction in burst release of F2 may be attributed to the covalently-linked PEG surface corona causing the production of a hydrophilic protective layer around the individual particles, impairing the release rate (Han et al., 2022). This falls in accordance with previously attempted studies in literature, whereby the effect of the logP of the API will alter the release kinetics, depending on LP surface properties (Shibata et al., 2015). In the case of the research within this study, the AMOX has a favourable association within the PEG surface chains due to its low logP, causing a slowing of the API release.

3.5. Cell attachment and viability studies

The in vitro attachment and viability assays performed here demonstrate the suitability of the formulations for use as a therapeutic treatment. These experiments allow an assessment of the physical and physiological health of cells in response to treatment with the range of formulations described here. Results from the crystal violet attachment assay show that at 4 h the presence of F1 and F2, both empty and API loaded, did not have any negative effect on the cellular attachment when compared to the control. This is an important property to assess for application in scaffold systems for API delivery and tissue repair, as the adhesion of cells at implant surfaces is essential in controlling mechanisms of signal transduction between cells and ensuring the induction of a biological response (Rychly and Nebe, 2009). This research shows that the initial attachment of osteoblast-like cells is not significantly affected by the presence of any of the liposomal formulations discussed here. Fig. 6a, shows no significant difference in the recorded absorbance between the positive control and any of the LP formulation samples. Representative phase contrast images, Fig. 6b–e, show similar morphology of attached cells on all samples. Some isolated rounded cells can be seen on all of the samples which is characteristic of the very initial stages of cellular attachment (Lavenus et al., 2011). However, on all samples, small islands of cells are observed indicative of early proliferative stages.

The MTT results demonstrate no cytotoxic effect of the control LPs or AMOX groups on the U2OS model cell line. Optical densities presented no significant change in the presence of the LP formulations when compared to the positive control, suggesting similar levels of metabolic activity in all sample groups (Fig. 7a). When calculated as percentage viability, with a positive control on standard tissue culture plastic with no liposomal addition considered as 100% viable, at day 7 the viability in groups containing LPs ranged from 97 to 100% (Fig. 7b). Interestingly at all timepoints the empty LPs presented with slightly lower viability than those containing the AMOX. Here, it is hypothesised that this is due to a marginally higher degree of ethanol incorporation during the empty LP formulation as the aqueous phase used was blank PBS (Elsana et al., 2019), causing a slight decrease in viability. It should be noted that this difference is not statistically significant.

When considering the release profile of AMOX from both F1 and F2, an average of 88 % of the drug is released within the initial 3 days, meaning that any potential effect of the API on cells should be experienced within this time frame. Therefore, the results obtained here suggest that the AMOX loaded LPs can successfully deliver the API without invoking any cytotoxic effects on cells especially as within an in vivo system there would be a degree of API clearance by metabolic pathways, reducing AMOX build up within a localised area. It is apparent that within simulated in vitro conditions, the PEGylation of a phospholipid

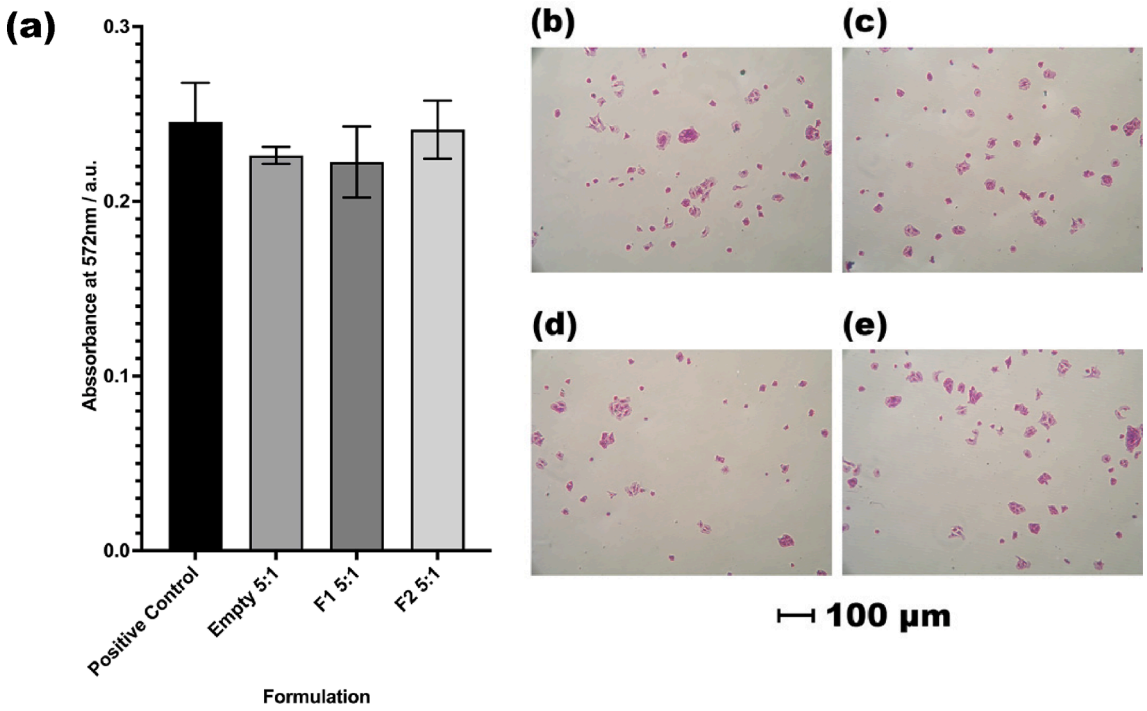

Fig. 6. Crystal violet attachment assay data, (a) mean absorbance values obtained for each sample group, (b–e) phase contrast images showing the distribution and morphology of attached cells at 4 h after seeding with media containing liposomal formulations. (For interpretation of the references to colour in this figure legend, the reader is referred to the web version of this article.)

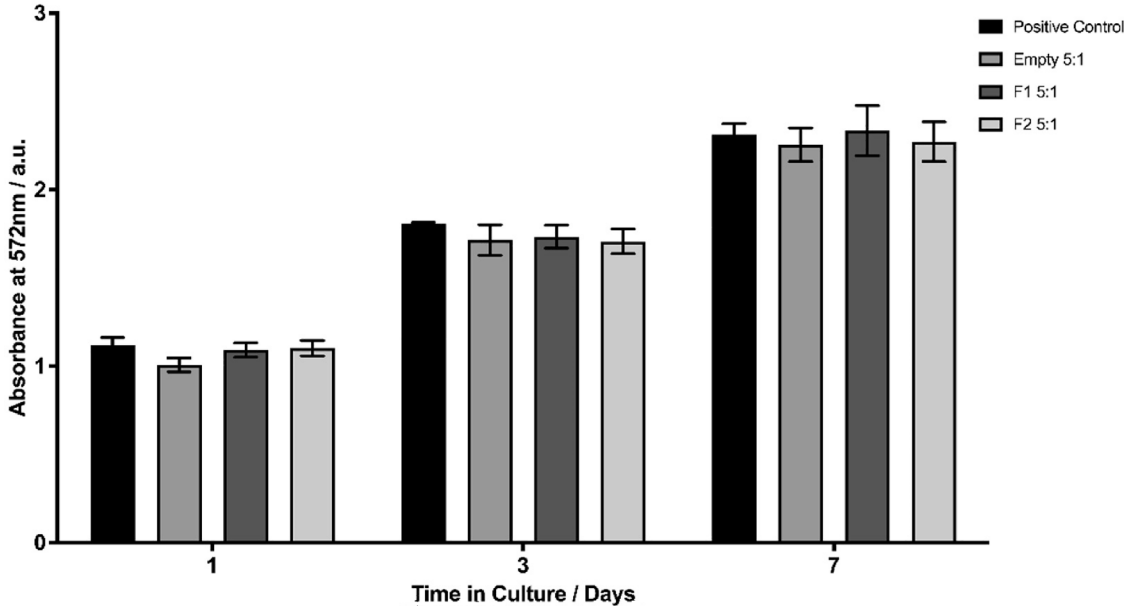

Fig. 7. MTT viability assay data showing mean absorbance values obtained for each sample group of U2OS cells when cultured in the presence of each liposomal formulation.

doesn't affect the viability of the model cell line.

3.6. Bacterial studies

3.6.1. MIC and MBC determination

The determined MIC and MBC values, as displayed in table SI 3 and table SI 4, a slightly more potent efficacy against *P. mirabilis* as opposed to *S. aureus* is witnessed. It is apparent that the addition of PEG within the formulation has a negligeable effect upon the bactericidal efficacy of the API, as both F1 and F2 share the same MIC values for both the Gram positive and negative bacteria used in this study. The MIC levels fall within an expected range compared to other studies performed (Mlynek et al., 2016). The slight difference in MBC levels between the Gram positive and negative bacteria could possibly lead to a "selective" preference in bactericidal activity against *P. mirabilis*, which may allow for the increased viability of *S. aureus* growth. To address this issue, further work may be needed to ensure equal potency against both Gram positive and negative, to ensure the treatment regimens are not complicated by

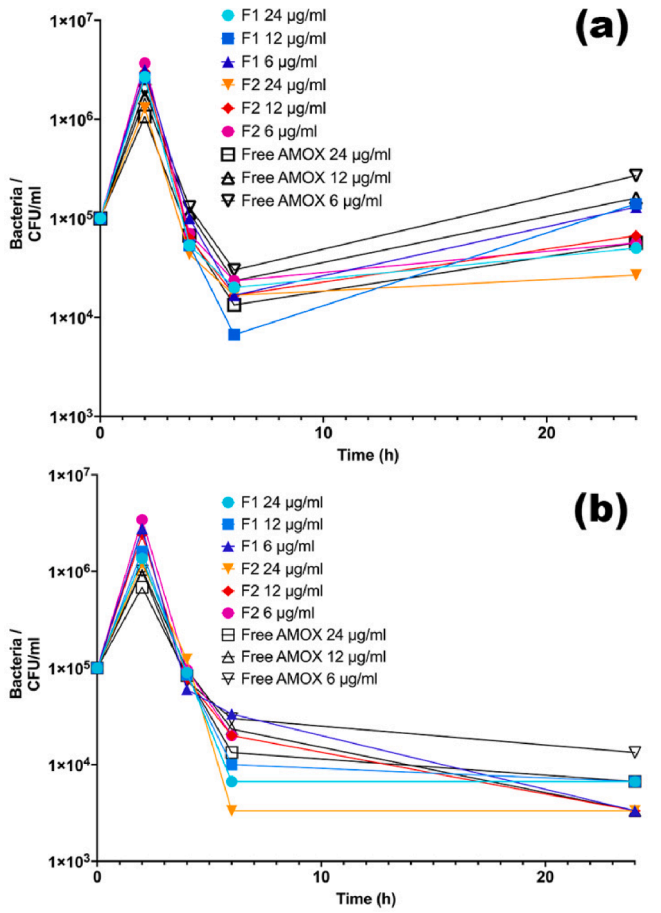

Fig. 8. Time kill assay data displayed over a 24-hour period for (a) *S. aureus* and (b) *P. mirabilis*.

this issue. Despite this, the payload delivered from the LPs in vitro would suggest that the concentration of API released would be far greater than that of the MBC, reducing the risk of selective "man-made" bacterial growth occurring; AMOX is a broad-spectrum AB, therefore, the key issue to consider is ensuring the API concentration remains lethal to both Gram positive and Gram negative. This factor is further analysed within the 24-hour time kill assay performed. The MBC of all formulations against *P. mirabilis* was 6 µg/ml. Against *S. aureus*, F1 and unencapsulated AMOX had an MBC of 12 µg/ml and F2 had an MBC of 6 µg/ml.

3.6.2. Time-Kill assay

The findings of the time kill assay, displayed in Fig. 8, display a differing antibiotic efficacy profile between Gram positive and Gram negative bacteria over a 24-hour period. At the 6-hour time period, the antibacterial efficacy appeared similar, reducing the apparent bacterial load within the range of 99.5–99.9% from the original 1×10^5 CFU/ml concentration. At the 24-hour timepoint, the CFU/ml for *S. aureus* increases, displaying a lack of bacterial eradication and a stoppage in antibacterial efficacy of the AMOX. This is hypothesised to be caused by the development of AMR during the assay. This can occur when the drug release rate is insufficient to maintain above-MIC concentrations of the API, which then allows the bacterial growth rate to exceed the bacterial death rate. As stated in previously conducted literature, the emergence of methicillin resistant *S. aureus* (MRSA) species is a common development caused by the upregulation of genes such as *mecA* and *femX* (Yao et al., 2019), and can lead to the cessation of AMOX efficacy. It's possible that the isolation of these colonies after AMOX treatment is the reason for the increase in CFU/ml over the duration between 6 and 24 h. This issue is particularly poignant when using AB concentrations within a narrow range of the predetermined MIC (Yao et al., 2019). As stated previously, the concentrations delivered by the full-dose LP formulations would likely be far greater than the concentrations used for this representative time kill assay, hence decreasing the risk of the development of resistance. The assay performed used concentrations of API at maximum 4× the MIC and were still capable of displaying a decrease beyond the original bacterial density. This would be an indicator that concentrations above these would provide a bactericidal effect, rather than just inhibitory.

This issue wasn't experienced for the Gram negative *P. mirabilis*, as positive bacterial growth was inhibited for all formulations over the 24-hour time period. As expected, the highest concentration used, 24 µg/ml (4 × MIC), provided the most effective antibacterial efficacy in most cases. A similar pattern for all formulations, both Gram positive and negative, indicating an increase in CFU/ml at the 2 h timepoint, which is consistent for the lag-time exhibited by market-available AMOX products (Li et al., 2016).

In general, the liposomal formulations, F1 and F2, appeared to have a better prolonged antibacterial effect compared to the unencapsulated AMOX. It is apparent that the burst release profile exhibited by the LPs, as displayed in figure 5, releases a sufficient therapeutic concentration of AMOX to eradicate bacteria at the same level as free AMOX. Additionally, the release profile exhibited by the LPs provides an extended duration of antimicrobial efficacy, as displayed the decreasing CFU/ml between the 6- and 24-hour timepoints. There are no statistically relevant differences in the antimicrobial efficacy seen between F1 and F2 at each given timepoint, which is expected given the similar drug release profiles.

4. Considerations of anti-PEG antibodies

As mentioned during the introduction, the issue of APAs has become of increasing interest during recent years, especially given the increasing occurrence of PEG being used within pharmaceutical formulations (Zalba et al., 2022). APAs are IgM and IgG antibodies produced either naturally within the body, or as a result of exposure to PEG, which target and bind specifically to PEG moieties, causing a variety of downstream immunoresponses. Within this section, it will be discussed whether the advantages of employing the pharmaceutical properties of PEG outweigh its associated drawbacks or not.

The addition of PEG to pharmaceutical formulations has been attributed to reducing immunogenicity and increasing formulation circulation via a reduced rate of clearance (Shi et al., 2022). Most nanomedicines approved for market use currently employ PEG as part of their material composition (Shi et al., 2022), most notably being used within the recent Covid-19 lipid NP vaccine. The PEG coating can help disguise the nanovessels from the body's natural immunoreceptors, such as within the mononuclear phagocyte system (MPS) (Gordon and Plüddemann, 2019), which will usually cause an increased rate of clearance for nanoformulations. For fast-delivery nanoparticles, which may be used mainly for targeted delivery instead of prolonged delivery, this factor may not be an issue, as the payload of the NP will be delivered prior to the MPS clearance. For prolonged delivery LPs, avoidance of clearing systems, including the MPS, may be favourable as it allows the API to be delivered over an increased duration of time. The lack of immunogenicity is due mainly to PEG causing the blockage and inhibition of various degradative enzymes (Chen et al., 2021). PEG is a non-toxic material which has gained approval for use by the Food and Drug Administration (FDA), the Medicines and Healthcare Products Regulatory Agency (MHRA) and the European Medicines Agency (EMA).

The drawbacks to the use of PEG come mainly in the form of APAs. APAs can invoke neutralisation of the NP, enhanced formulation clearance and possible hypersensitivity reactions. A recent study estimated 20–70% of humans possess APAs (Grenier et al., 2023), making it a non-negligible factor to consider, however, this still leaves a large population group which don't possess APAs. Daily exposure to PEG is relatively

common, as it is frequently found in cosmetic products such as moisturisers. The daily use could lead to a pre-existing population of APAs, even without receiving a systemic concentrated dose, such as via a pharmaceutical formulation e.g., PEGylated vaccine (Kozma et al., 2020).

Increased formulation clearance due to APAs is an interesting factor to consider, as PEGylation is often credited with decreasing the rate of clearance. However, in the presence of APAs, a phenomenon known as accelerated blood clearance (ABC) can occur, whereby the opsonin IgM triggers a catalytic pathway leading to the subsequent activation of endocytic and phagocytic processes (Abu Lila et al., 2013). Hypersensitivity to PEGylated nanomedicines can also be caused by the activation of APAs, causing a range of adverse reactions including hypotension, breathing difficulties, and in extreme cases, death (Chen et al., 2023). A direct link between both IgG and IgM anti-PEG antibody activation has been linked to the causation of hypersensitive reactions, due to the instigation of immune cells such as neutrophils and basophils (Chen et al., 2023).

Considering the facts presented above, the authors would still surmise that the benefits of the addition of PEG to the formulations synthesised in this study would negate the negative factors that can occur as a result of APAs. The improved physical properties of the formulation, including a reduction in particle size and improved stability, along with a more-controlled API release profile are desirable assets to possess. In addition, the presence of a PEG moiety improves the capacity for the formation of more complex DDSs, such as protein-conjugated LPs or LP-scaffold complexes. The risks of adverse reactions as a result of APAs are often mitigated by the potential healthcare benefits that can be gained by the proper delivery of the API, which is one of the main reasons that many of the approved NP-based medicines incorporate PEG within their design (Wang et al., 2022). The delivery of the API and subsequent antimicrobial efficacy in this study showed comparable data, indicating that the addition of PEG doesn't overall hinder the formulation's effectiveness in this study.

The question arises as to what alternatives may be available to help replace PEG, or whether an alternative is even needed. There is currently research looking into the use of other hydrophilic polymers such as alternatively-branched poly(glycerol)s, poly(acrylamide)s and hyaluronic acid, to maintain the stealth properties displayed by PEGylated LPs, without the risk of activating APAs (Hoang Thi et al., 2020). The use of zwitterionic polymers, including poly(carboxybetaine) and poly (carboxybetaine methacrylate) are also potential candidates for replacing PEG(Hoang Thi et al., 2020). Whilst many of the candidates show potential as alternatives, it should be noted that none have been found yet to be a perfect replacement.

5. Conclusions

Using MFs, the first instance of the liposomal encapsulation of AMOX has been displayed, producing LPs with promising physical characteristics and antibacterial efficacy. The capacity to produce a formulation which can lower the required dose of AB could help reduce the instances of AMR, due to a reduced amount of API reaching unintended target areas.

The requirement of PEG within this formulation is also evaluated, based upon the changes in the formulation seen after the addition of PEG. A review of literature suggests that whilst alternative moieties are currently being investigated to replace PEG, none have yet come into fruition as a viable successor due to issues of synthesis, pharmacokinetics and cost (Hoang Thi et al., 2020). It is summarised that the inclusion of PEG is beneficial within the liposomal formulation, as multiple aspects of the formulation are improved, including the stability, modified API release profile, and the capacity to further modify the membrane e.g., with protein conjugates. Future work planned to further enhance the selective delivery of AMOX involves the coupling of the liposomes with other DDSs, including electrospun API-eluting fibre scaffolds.

Author Contributions

Edward Weaver – Conceptualisation, Data curation, Formal Analysis, Methodology, Investigation, Writing – original draft, Writing – Review and editing. **Robyn Macartney** - Data curation, Formal Analysis, Methodology, Investigation, Writing – original draft, Writing – Revie w and editing. Robyn Irwin – Methodology, Writing – review and editing. **Shahid Uddin** – Funding acquisition, Writing – review and editing. **Andrew Hooker** - Funding acquisition, Writing – review and editing. **George A. Burke** – Methodology, Supervision, Writing – review and editing. **Matthew P Wylie** – Methodology, Writing – review and editing. **Dimitrios A. Lamprou** – Conceptualisation, Funding acquisition, Supervision, Writing – review and editing.

Funding

This research was funded by Immunocore.

CRediT authorship contribution statement

Edward Weaver: Conceptualisation, Data curation, Formal Analysis, Methodology, Investigation, Writing – original draft, Writing – Review and editing. **Robyn A. Macartney:** Data curation, Formal Analysis, Methodology, Investigation, Writing – original draft, Writing – Revie w and editing. **Robyn Irwin:** Methodology, Writing – review and editing. **Shahid Uddin:** Writing – review & editing, Supervision, Resources. **Andrew Hooker:** Writing – review & editing, Supervision, Funding acquisition. **George A. Burke:** Writing – review & editing, Supervision. **Matthew P. Wylie:** Methodology, Writing – review and editing. **Dimitrios A. Lamprou:** Conceptualisation, Funding acquisition, Supervision, Writing – review and editing..

Declaration of Competing Interest

The authors declare that they have no known competing financial interests or personal relationships that could have appeared to influence the work reported in this paper.

Data availability

Data will be made available on request.

Appendix A. Supplementary material

Supplementary data to this article can be found online at https://doi.org/10.1016/j.ijpharm.2023.123710.

References

Alinaghi, A., Rouini, M.R., Johari daha, f. & moghimi, h. r., 2014. The influence of lipid composition and surface charge on biodistribution of intact liposomes releasing from hydrogel-embedded vesicles. Int. J. Pharm. 459, 30–39.

Baby, T., Liu, Y., Yang, G., Chen, D., Zhao, C.-X., 2021. Microfluidic synthesis of curcumin loaded polymer nanoparticles with tunable drug loading and pH-triggered release. J. Colloid Interface Sci. 594, 474–484.

Ballacchino, G., Weaver, E., Mathew, E., Dorati, R., Genta, I., Conti, B., Lamprou, D.A., 2021. Manufacturing of 3D-Printed Microfluidic Devices for the Synthesis of Drug-Loaded Liposomal Formulations. Int. J. Mol. Sci. 22, 8064.

Banerjee, U., Wolfe, S., O'Boyle, Q., Cuddington, C., Palmer, A.F., 2022. Scalable production and complete biophysical characterization of poly (ethylene glycol) surface conjugated liposome encapsulated hemoglobin (PEG-LEH). PLoS One 17, e0269939.

Bassetti, S., Tschudin-Sutter, S., Egli, A., Osthoff, M., 2022. Optimizing antibiotic therapies to reduce the risk of bacterial resistance. Eur. J. Intern. Med.

Bebu, A., Szabó, L., Leopold, N., Berindean, C., David, L., 2011. IR, Raman, SERS and DFT study of amoxicillin. J. Mol. Struct. 993, 52–56.

Canaparo, R., Foglietta, F., Giuntini, F., Della pepa, c., dosio, f. & serpe, l., 2019. Recent developments in antibacterial therapy: Focus on stimuli-responsive drug-delivery systems and therapeutic nanoparticles. Molecules 24, 1991.
Cannito, S., Bincoletto, V., Turato, C., Pontisso, P., Scupoli, M.T., Ailuno, G., Andreana, I., Stella, B., Arpicco, S., Bocca, C., 2022. Hyaluronated and PEGylated Liposomes as a Potential Drug-Delivery Strategy to Specifically Target Liver Cancer and Inflammatory Cells. Molecules 27, 1062.
Chang, C., Meikle, T.G., Su, Y., Wang, X., Dekiwadia, C., Drummond, C.J., Conn, C.E., Yang, Y., 2019. Encapsulation in egg white protein nanoparticles protects anti-oxidant activity of curcumin. Food Chem. 280, 65–72.
Chen, W.-A., Chang, D.-Y., Chen, B.-M., Lin, Y.-C., Barenholz, Y., Roffler, S.R., 2023. Antibodies against Poly(ethylene glycol) Activate Innate Immune Cells and Induce Hypersensitivity Reactions to PEGylated Nanomedicines. ACS Nano 17, 5757–5772.
Chen, B.M., Cheng, T.L., Roffler, S.R., 2021. Polyethylene Glycol Immunogenicity: Theoretical, Clinical, and Practical Aspects of Anti-Polyethylene Glycol Antibodies. ACS Nano 15, 14022–14048.
Chen, W., Duša, F., Witos, J., Ruokonen, S.-K., Wiedmer, S.K., 2018. Determination of the main phase transition temperature of phospholipids by nanoplasmonic sensing. Sci. Rep. 8, 14815.
Dave, V., Gupta, A., Singh, P., Gupta, C., Sadhu, V., Reddy, K.R., 2019. Synthesis and characterization of celecoxib loaded PEGylated liposome nanoparticles for biomedical applications. Nano-Structures & Nano-Objects 18, 100288.
Ekonomou, s. i., akshay thanekar, p., lamprou, d. a., weaver, e., doran, o. & stratakos, a. c., 2022. Development of Geraniol-Loaded Liposomal Nanoformulations against Salmonella Colonization in the Pig Gut. J. Agric. Food Chem. 70, 7004–7014.
Elsana, H., Olusanya, T.O., Carr-Wilkinson, J., Darby, S., Faheem, A., Elkordy, A.A., 2019. Evaluation of novel cationic gene based liposomes with cyclodextrin prepared by thin film hydration and microfluidic systems. Sci. Rep. 9, 15120.
Foerster, S., Unemo, M., Hathaway, L.J., Low, N., Althaus, C.L., 2016. Time-kill curve analysis and pharmacodynamic modelling for in vitro evaluation of antimicrobials against Neisseria gonorrhoeae. BMC Microbiol. 16.
Ghaferi, M., Raza, A., Koohi, M., Zahra, W., Akbarzadeh, A., Ebrahimi shahmabadi, h. & alavi, s. e., 2022. Impact of PEGylated Liposomal Doxorubicin and Carboplatin Combination on Glioblastoma. Pharmaceutics 14, 2183.
González-Plaza, J.J., Blau, K., Milaković, M., Jurina, T., Smalla, K., Udiković-Kolić, N., 2019. Antibiotic-manufacturing sites are hot-spots for the release and spread of antibiotic resistance genes and mobile genetic elements in receiving aquatic environments. Environ. Int. 130, 104735.
Gordon, S., Plüddemann, A., 2019. The mononuclear phagocytic system. Generation of diversity. *Frontiers in immunology* 10, 1893.
Grenier, P., Chénard, V., Bertrand, N., 2023. The mechanisms of anti-PEG immune response are different in the spleen and the lymph nodes. J. Control. Release 353, 611–620.
Han, X., Zhang, Y., Tian, J., Wu, T., Li, Z., Xing, F., Fu, S., 2022. Polymer-based microfluidic devices: A comprehensive review on preparation and applications. Polym. Eng. Sci. 62, 3–24.
Hoang thi, t. t., pilkington, e. h., nguyen, d. h., lee, j. s., park, k. d. & truong, n. p., 2020. The importance of poly (ethylene glycol) alternatives for overcoming PEG immunogenicity in drug delivery and bioconjugation. Polymers 12, 298.
Jaradat, E., Weaver, E., Meziane, A., Lamprou, D.A., 2022. Microfluidic paclitaxel-loaded lipid nanoparticle formulations for chemotherapy. Int. J. Pharm. 628, 122320.
Ju, Y., Carreño, J.M., Simon, V., Dawson, K., Krammer, F., Kent, S.J., 2023. Impact of anti-PEG antibodies induced by SARS-CoV-2 mRNA vaccines. Nat. Rev. Immunol. 23, 135–136.
Kaddah, S., Khreich, N., Kaddah, F., Charcosset, C., Greige-Gerges, H., 2018. Cholesterol modulates the liposome membrane fluidity and permeability for a hydrophilic molecule. Food Chem. Toxicol. 113, 40–48.
Kozma, G.T., Shimizu, T., Ishida, T., Szebeni, J., 2020. Anti-PEG antibodies: Properties, formation, testing and role in adverse immune reactions to PEGylated nano-biopharmaceuticals. Adv. Drug Deliv. Rev. 154–155, 163–175.
Lavenus, S., Pilet, P., Guicheux, J., Weiss, P., Louarn, G., Layrolle, P., 2011. Behaviour of mesenchymal stem cells, fibroblasts and osteoblasts on smooth surfaces. Acta Biomater 7, 1525–1534.
Li, B., Qiu, Y., Shi, H., Yin, H., 2016. The importance of lag time extension in determining bacterial resistance to antibiotics. Analyst 141, 3059–3067.
Lila, A.B.U., A. s., kiwada, h. & ishida, t., 2013. The accelerated blood clearance (ABC) phenomenon: Clinical challenge and approaches to manage. J. Control. Release 172, 38–47.
Marcel, S., Tito, U., Ines, I., Pierre, N.J., 2018. Validation of HPLC-UV method for determination of amoxicillin Trihydrate in capsule. Annals of Advances in Chemistry 2, 055–072.
Maritim, S., Boulas, P., Lin, Y., 2021. Comprehensive analysis of liposome formulation parameters and their influence on encapsulation, stability and drug release in glibenclamide liposomes. Int. J. Pharm. 592, 120051.
Mlynek, K.D., Callahan, M.T., Shimkevitch, A.V., Farmer, J.T., Endres, J.L., Marchand, M., Bayles, K.W., Horswill, A.R., Kaplan, J.B., 2016. Effects of low-dose amoxicillin on Staphylococcus aureus USA300 biofilms. Antimicrob. Agents Chemother. 60, 2639–2651.
Nakhaei, P., Margiana, R., Bokov, D.O., Abdelbasset, W.K., Jadidi Kouhbanani, M.A., Varma, R.S., Marofi, F., Jarahian, M., Beheshtkhoo, 2021. Liposomes: structure, biomedical applications, and stability parameters with emphasis on cholesterol. Front Bioeng Biotechnol 9, 705886.
Patel, A., Dey, S., Shokeen, K., Karpiński, T.M., Sivaprakasam, S., Kumar, S., Manna, D., 2021. Sulfonium-based liposome-encapsulated antibiotics deliver a synergistic antibacterial activity. RSC Med. Chem. 12, 1005–1015.
Radyukevich, D., Akulova, V., Melnikova, G., Chizhik, S., Ting, N. T., Bing, N. T., 2019. Properties and structure of gelatin composite films with amoxicillin microparticles. Journal of Physics: Conference Series. IOP Publishing, 012064.
Richtering, W., Alberg, I., Zentel, R., 2020. Nanoparticles in the biological context: surface morphology and protein corona formation. Small 16, 2002162.
Rychly, J., Nebe, B., 2009. Interface biology of implants. Cell Adh. Migr. 3, 390–394.
Shi, D., Beasock, D., Fessler, A., Szebeni, J., Ljubimova, J.Y., Afonin, K.A., Dobrovolskaia, M.A., 2022. To PEGylate or not to PEGylate: Immunological properties of nanomedicine's most popular component, polyethylene glycol and its alternatives. Adv. Drug Deliv. Rev. 180, 114079.
Shibata, H., Izutsu, K.-I., Yomota, C., Okuda, H., Goda, Y., 2015. Investigation of factors affecting in vitro doxorubicin release from PEGylated liposomal doxorubicin for the development of in vitro release testing conditions. Drug Dev. Ind. Pharm. 41, 1376–1386.
Sommonte, F., Weaver, E., Mathew, E., Denora, N., Lamprou, D.A., 2022. In-house innovative "Diamond Shaped" 3D printed microfluidic devices for lysozyme-loaded liposomes. Pharmaceutics 14, 2484.
Tavares, A.G., Andrade, J., Silva, R.R.A., Marques, C.S., da Silva, J.O.R., Vanetti, M.C.D., de Melo, N.R., Soares, N.D.F.F., 2021. Carvacrol-loaded liposome suspension: Optimization, characterization and incorporation into poly (vinyl alcohol) films. Food Funct. 12, 6549–6557.
Tong, S., Pan, J., Lu, S., Tang, J., 2018. Patient compliance with antimicrobial drugs: a Chinese survey. Am. J. Infect. Control 46, e25–e9.
Trucillo, P., Ferrari, P.F., Campardelli, R., Reverchon, E., Perego, P., 2020. A supercritical assisted process for the production of amoxicillin-loaded liposomes for antimicrobial applications. J. Supercrit. Fluids 163, 104842.
Van Staa, T., LI, Y., Gold, N., Chadborn, T., Welfare, W., Palin, V., Ashcroft, D. M., Bircher, J., 2022. Comparing antibiotic prescribing between clinicians in UK primary care: an analysis in a cohort study of eight different measures of antibiotic prescribing. BMJ Quality & Safety, bmjqs-2020-0121.
Vijayakumar, M.R., Kosuru, R., Vuddanda, P.R., Singh, S.K., Singh, S., 2016. Trans resveratrol loaded DSPE PEG 2000 coated liposomes: an evidence for prolonged systemic circulation and passive brain targeting. J. Drug Delivery Sci. Technol. 33, 125–135.
Volk, A.A., Epps, R.W., Abolhasani, M., 2021. Accelerated development of colloidal nanomaterials enabled by modular microfluidic reactors: toward autonomous robotic experimentation. Adv. Mater. 33, 2004495.
Wang, S., Cheng, K., Chen, K., Xu, C., Ma, P., Dang, G., Yang, Y., Lei, Q., Huang, H., Yu, Y., Fang, Y., Tang, Q., Jiang, N., Miao, H., Liu, F., Zhao, X., Li, N., 2022. Nanoparticle-based medicines in clinical cancer therapy. Nano Today 45, 101512.
Wang, S., Chen, Y., Guo, J., Huang, Q., 2023. Liposomes for tumor targeted therapy: a review. Int. J. Mol. Sci. 24, 2643.
Weaver, E., Uddin, S., Cole, D.K., Hooker, A., Lamprou, D.A., 2021. The present and future role of microfluidics for protein and peptide-based therapeutics and diagnostics. Appl. Sci. 11, 4109.
Weaver, E., Mathew, E., Caldwell, J., Hooker, A., Uddin, S., Lamprou, D.A., 2022a. The manufacturing of 3D-printed microfluidic chips to analyse the effect upon particle size during the synthesis of lipid nanoparticles. J. Pharmacy Pharmacol.
Weaver, E., O'Connor, E., Cole, D.K., Hooker, A., Uddin, S., Lamprou, D.A., 2022b. Microfluidic-mediated self-assembly of phospholipids for the delivery of biologic molecules. Int. J. Pharm. 611, 121347.
Weaver, E., O'Hagan, C., Lamprou, D.A., 2022c. The sustainability of emerging technologies for use in pharmaceutical manufacturing. Expert Opin. Drug Deliv. 19, 861–872.
Wu, Y., Geng, J., Cheng, X., Yang, Y., Yu, Y., Wang, L., Dong, Q., Chi, Z., Liu, C., 2022. Cosmetic-derived mannosylerythritol lipid-b-phospholipid nanoliposome: an acid-stabilized carrier for efficient gastromucosal delivery of amoxicillin for in vivo treatment of helicobacter pylori. ACS Omega 7, 29086–29099.
Yao, Q., Gao, L., Xu, T., Chen, Y., Yang, X., Han, M., He, X., Li, C., Zhou, R., Yang, Y., 2019. Amoxicillin administration regimen and resistance mechanisms of staphylococcus aureus established in tissue cage infection model. Front. Microbiol. 10, 1638.
Zalba, S., ten Hagen, T.L., Burgui, C., Garrido, M.J., 2022. Stealth nanoparticles in oncology: facing the PEG dilemma. J. Control. Release 351, 22–36.
Zhang, Y., Mintzer, E., Uhrich, K.E., 2016. Synthesis and characterization of PEGylated bolaamphiphiles with enhanced retention in liposomes. J. Colloid Interface Sci. 482, 19–26.